RESEARCH ARTICLE

Human Mutation

OFFICIAL JOURNAL HGVS HUMAN GENOME VARIATION SOCIETY www.hgvs.org

Dynamin 2 Mutations Associated With Human Diseases Impair Clathrin-Mediated Receptor Endocytosis

Marc Bitoun,[1,2]* Anne-Cécile Durieux,[1,2] Bernard Prudhon,[1,2] Jorge A. Bevilacqua,[1,3] Adrien Herledan,[4] Vehary Sakanyan,[4,5] Andoni Urtizberea,[6] Luis Cartier,[7] Norma B. Romero,[1,2,8] and Pascale Guicheney[1,2,8]

[1]Institut National de la Santé et de la Recherche Médicale (INSERM), U582, Institut de Myologie, Paris, France; [2]Pierre and Marie Curie University (UPMC), Université Paris 06, Unité Mixte de Recherche (UMR)_S 582, Institut Française de la Recherche 14 (IFR14), Paris, France; [3]Departamento de Neurología y Neurocirugía, Hospital Clinico of University of Chile (HCUCH) and Instituto de Ciencias Biomédicas Universidad de Chile, Santiago, Chile; [4]Centre National de la Recherche Scientifique (CNRS), Unité Mixte de Recherche (UMR) 6204, Laboratoire de Biotechnologie, Université de Nantes, Nantes, France; [5]ProtNeteomix, Nantes, France; [6]Assistance Publique–Hôpitaux de Paris (AP-HP), Hôpital Marin, Hendaye, France; [7]Departamento de Ciencias Neurológicas, Facultad de Medicina, Universidad de Chile, Hospital del Salvador, Santiago, Chile; [8]Assistance Publique–Hôpitaux de Paris (AP-HP), Groupe Hospitalier Pitié-Salpêtrière, Service de Biochimie Métabolique, Paris, France

Communicated by Mireille Claustres

Received 17 November 2008; accepted revised manuscript 22 June 2009.
Published online 7 July 2009 in Wiley InterScience (www.interscience.wiley.com). DOI 10.1002/humu.21086

ABSTRACT: Dynamin 2 (DNM2) is a large GTPase involved in the release of nascent vesicles during endocytosis and intracellular membrane trafficking. Distinct DNM2 mutations, affecting the middle domain (MD) and the Pleckstrin homology domain (PH), have been identified in autosomal dominant centronuclear myopathy (CNM) and in the intermediate and axonal forms of the Charcot-Marie-Tooth peripheral neuropathy (CMT). We report here the first CNM mutation (c.1948G>A, p.E650K) in the DNM2 GTPase effector domain (GED), leading to a slowly progressive moderate myopathy. COS7 cells transfected with DNM2 constructs harboring a disease-associated mutation in MD, PH, or GED show a reduced uptake of transferrin and low-density lipoprotein (LDL) complex, two markers of clathrin-mediated receptor endocytosis. A decrease in clathrin-mediated endocytosis was also identified in skin fibroblasts from one CNM patient. We studied the impact of DNM2 mutant overexpression on epidermal growth factor (EGF)-induced extracellular signal-regulated kinase 1 (ERK1) and ERK2 activation, known to be an endocytosis- and DNM2-dependent process. Activation of ERK1/2 was impaired for all the transfected mutants in COS7 cells, but not in CNM fibroblasts. Our results indicate that impairment of clathrin-mediated endocytosis may play a role in the pathophysiological mechanisms leading to DNM2-related diseases, but the tissue-specific impact of DNM2 mutations in both diseases remains unclear.
Hum Mutat 30:1419–1427, 2009. © 2009 Wiley-Liss, Inc.

KEY WORDS: centronuclear myopathy; CMT; DNM2; neuropathy; clathrin; endocytosis; ERK1/2

Introduction

Dynamins belong to a superfamily of large GTPases that includes classical dynamins and several dynamin-like proteins [Praefcke and McMahon, 2004]. The three classical dynamins expressed in mammals are the neuron-specific dynamin 1 (MIM# 602377) [Shpetner and Vallee, 1989], the ubiquitously expressed dynamin 2 (MIM# 602378) [Cook et al., 1994; Diatloff-Zito et al., 1995], and dynamin 3 (MIM# 611445), which is expressed in brain, testis, and lung [Nakata et al., 1993]. Dynamin 2 (DNM2) is implicated in membrane trafficking [Warnock et al., 1997], where it acts as a mechanochemical scaffolding molecule that can hydrolyze GTP to deform biological membranes [Praefcke and McMahon, 2004]. DNM2 plays a role in membrane trafficking from both the plasma membrane [Warnock et al., 1997] and the trans-Golgi network [Jones et al., 1998], in formation of actin stress-fibers [Yoo et al., 2005], in actin-membrane interface assembly [Orth and McNiven, 2003], and in centrosome cohesion [Thompson et al., 2004]. Involvement of DNM2 in activation of the mitogen-activated protein kinases (MAPK) extracellular signal-regulated kinase 1 (ERK1) and ERK2 has also been reported [Kranenburg et al., 1999].

DNM2 is a 100-kDa multidomain protein composed of a N-terminal GTPase domain, a middle domain (MD), a pleckstrin homology domain (PH), a GTPase effector domain (GED), and a C-terminal proline rich domain (PRD). During the last 5 years, *DNM2* mutations have been identified in two distinct clinical presentations: autosomal dominant centronuclear myopathy (AD-CNM; MIM# 160150) [Bitoun et al., 2005, 2007, 2009; Echaniz-Laguna et al., 2007; Schessl et al., 2007], and dominant intermediate and axonal Charcot-Marie-Tooth disease (CMT; MIM# 606482) [Züchner et al., 2005; Fabrizi et al., 2007; Bitoun et al., 2008; Gallardo et al., 2008]. DNM2-related CNM is a slowly progressive congenital myopathy characterized by frequent centrally located nuclei in muscle fibers. The most frequent clinical features are delayed motor milestones, facial and generalized muscle weakness, ptosis, and ophthalmoplegia [Fischer et al., 2006]. Nevertheless, the severity of DNM2-related CNM is variable, including a wide spectrum of phenotypes, ranging from severe neonatal to mild late-onset familial forms [Bitoun et al., 2005, 2007, 2009; Echaniz-Laguna et al., 2007; Schessl et al., 2007]. DNM2-related CNM is a peripheral neuropathy characterized by

Additional Supporting Information may be found in the online version of this article.

*Correspondence to: Dr. Marc Bitoun, INSERM UMR_S 974, Institut de Myologie, Groupe Hospitalier Pitié-Salpêtrière, 75013, Paris, France.
E-mail: m.bitoun@institut-myologie.org

© 2009 WILEY-LISS, INC.

progressive muscle weakness and atrophy. In the axonal form of the disease, the nerve conduction velocity is usually normal (>38 m/s for the median nerve, which represents the cutoff value between the demyelinating CMT1 and the axonal CMT2). In the rare group of patients affected by dominant intermediate CMT, the nerve conduction velocity values are intermediate (between 25 and 45 m/s). Clinical overlap could exist in some CNM patients showing a mild axonal peripheral nerve involvement [Fischer et al., 2006], but the majority of patients seem to be affected by a tissue-specific disorder targeting either skeletal muscle or peripheral nerve. Until now, the 12 reported CNM-DNM2 mutations were located in either the MD or in the PH domain. In CMT, five distinct CMT-mutations have been identified in the N-terminal region of the PH domain, and more recently one in the MD [Gallardo et al., 2008]. To date, there is no mutation common to these two disorders and the underlying pathophysiological mechanisms remain unknown.

Here, we report the first CNM-DNM2 mutation (p.E650 K) affecting the GED, which causes a mild childhood-onset myopathy with a slow progressive course. We assessed the effect of overexpression of DNM2 mutants in COS7 cells on receptor-mediated endocytosis and epidermal growth factor (EGF)-induced ERK1 and ERK2 activation, which is an endocytosis and DNM2-dependent process [Andresen et al., 2002; Kranenburg et al., 1999]. We tested three CNM-DNM2 mutations located in the various DNM2 domains involved to date. The p.R465W mutation in the MD is the most frequent mutation in CNM patients. The p.V625del belongs to the group of mutations of the PH domain associated with a severe neonatal phenotype. The p.E650 K represents the first mutation identified in the GED. For comparison, we included a CMT-associated mutation (p.K562E) in the PH domain. We show that the overexpression of the disease-associated DNM2 mutants results in an impairment of clathrin-mediated receptor endocytosis. Similar impairment was found in fibroblasts from one CNM patient harboring the p.R465W mutation. The three CNM-DNM2 mutants and the CMT-DNM2 mutant induce similar inhibition of the MAPK ERK1 and ERK2 pathway in transfected cells. Our results suggest that an impairment of the membrane trafficking process contributes to the pathogenesis of both disorders. However, the specific causes of the skeletal muscle vs. peripheral nerve phenotypes remain to be determined.

Materials and Methods

DNM2 Sequencing

Screening for *DNM2* mutation was performed in one autosomal dominant CNM family from Chile including five affected patients (from 17 to 60 years old) in two generations. Clinical and morphological findings of the patients have already been described [Cartier and Hernandez, 1996]. DNA was extracted from blood samples and the 22 exons and intron–exon boundaries of the *DNM2* gene (NC_000019.8) were sequenced as previously reported [Bitoun et al., 2005]. The primer sequences are available on request. Nucleotide numbering reflects cDNA numbering with +1 corresponding to the A of the ATG translation initiation codon in the DNM2 isoform 1 reference sequence (NM_001005360). Amino acid numbering also corresponds to the DNM2 isoform 1 reference sequence (NP_001005360).

Cell Culture, Constructs, and Transfection

The COS7 cell line, skin fibroblasts from a CNM patient harboring the p.R465W DNM2 mutation (c.1393C>T; skin biopsy at the age of 30 years), and skin fibroblasts from healthy subjects (biopsied at the ages of 26 and 30 years for controls 1 and 2) were cultured in Dulbecco's modified Eagle's medium (DMEM) supplemented with 10% fetal calf serum (FCS) in a 5% CO_2 incubator at 37°C. The p.R465W fibroblast cell line was obtained from a patient of a previously reported large autosomal dominant CNM family (Family 1 in Jeannet et al. [2004] and in Bitoun et al. [2005]). The open reading frame of the wild-type DNM2 isoform 1 was generated by RT-PCR from lymphocyte mRNA and inserted in frame with the green fluorescent protein (GFP) in pGFP-NT-TOPO-TA vector (Invitrogen, Cergy, France). All the mutated plasmids were generated from this pGFP-wild-type DNM2 plasmid by directed mutagenesis using the Quick-Change Site-Directed Mutagenesis Kit (Stratagene, Amsterdam, The Netherlands). The p.K44A, p.R465W, p.K562E, p.V625del, and p.E650K were generated by nucleotide substitution or deletion; i.e., c.130_131AA>CG, c.1393C>T, c.1684A>G, c.1856_1875delGTC, and c.1948G>A, respectively. COS7 cells were seeded in 35-mm-diameter plates and transfected at 50% confluency using polyethylenimine (PEI). Then, 1 µg of plasmid and 2 µl of PEI (0.9 mg/ml) were mixed for 30 min in 200 µl DMEM and then added to cells for 4 hr at 37°C in a final volume of 1 ml. This medium was then replaced by DMEM-10% FCS for 2 days. In experiments with EGF stimulation, culture medium was replaced by DMEM without FCS 24 hr before treatment.

DNM Isoforms in Human Tissues and Skin Fibroblasts

Muscle RNA was extracted from a biopsy performed in the deltoid muscle of a 40-year-old healthy subject. In the absence of normal nerve biopsy, peripheral nerve RNA was extracted from the sensory superficial peroneal nerve of a 56-year-old patient affected by amyotrophic lateral sclerosis without peripheral sensory nerve involvement under electrophysiological and neuropathological examination. Fibroblast RNA was extracted from skin fibroblasts and whole-brain total RNA was commercially available (Clontech, Saint Germain en Laye, France). RNA extraction was done using Trizol reagent (Invitrogen). Total RNA (800 ng) was used as a template for reverse transcription (RT) and polymerase chain reaction (PCR). RT was performed using the Superscript II reverse transcriptase kit (Invitrogen) and PCR with Taq Platinum (Invitrogen) following the manufacturer's instructions. For DNM2, the forward primer was designed in exon 9 (5′-GGTGAAGATGGAGTTTGACGA-3′) and the reverse primer in exon 14 (5′-ATGAAAGGCGGCTCCAAG-3′). RT-PCR products were digested using BsaMI restriction enzyme (Promega, Charbonnieres, France). Products of digestion were separated on MetaPhor high resolution agarose gel (Tebu-bio, Le Perray en Yvelines, France). For amplification of DNM1 and DNM3 transcripts, the primers were as follows: DNM1-forward: 5′-GCT GTCTGTGGACAACCTCA-3′; DNM1-reverse: 5′-CACGGTCTT GTTGACAATGG-3′; DNM3-forward: 5′-AATTCCGAGCTCCTA GCACA-3′; and DNM3-reverse: 5′-TTAGTGTTGGCCTCC TTTGG-3′.

Immunocytochemistry

Fibroblasts were washed in phosphate buffered saline (PBS; 140 mM NaCl, 10 mM phosphate buffer, and 3 mM KCl, pH 7.4) and then fixed 20 min at −20°C in acetone for DNM2 immunostaining or 10 min at room temperature in 4% paraformaldehyde for transferrin receptor (TR) immunostaining. Nonspecific sites were blocked in PBS with 5% FCS and 0.01%

Triton X-100 for 90 min and incubated overnight with the goat polyclonal antibody C18 directed against human DNM2 (1:200; Santa Cruz Biotechnology, Santa Cruz, CA) or with the rabbit polyclonal antibody directed against TR (ab65831, 1:200; Abcam, Cambridge, UK). After washing, immunostaining was revealed by incubation for 2 hr with an anti-goat antibody- or anti-rabbit antibody-AlexaFluor 488 (Invitrogen) diluted at 1:200 in blocking buffer. Labeled cells were visualized by fluorescence microscopy (Axiophot system; Zeiss, Le Pecq, France) coupled with a charge-coupled device (CCD) camera and images were acquired using the Metaview software (Universal Imaging, Roper Scientific, Evry, France).

Endocytosis Assay

Transfected COS7 or fibroblasts were cultured in DMEM at 37°C for 45 min. In COS7 cells, transferrin-AlexaFluor 568 (Invitrogen) was added at 20 μg/ml at 37°C for 5 min or 15 min and low-density lipoprotein (LDL) complex–DiI conjugated (DiI-LDL; Invitrogen) was added at 15 μg/ml at 37°C for 15 min. Cells were washed three times with PBS and fixed in 4% paraformaldehyde before analysis using a confocal Leica SP2 microscope (Leica, Nanterre, France). The transferrin- or LDL-associated signal was measured in transfected cells (i.e., GFP-positive cells) using ImageJ software (NIH; http://rsbweb.nih.gov/ij) and the statistical significance was tested using a Student's *t*-test. In fibroblasts, biotinylated-transferrin (20 μg/ml) was added at 37°C for 5 min before washing in DMEM pH 2 and PBS. Cells were lysed in PBS by sonication and proteins were submitted to sodium dodecyl sulfate-polyacrylamide gel electrophoresis (SDS-PAGE), and then transferred onto polyvinylidene difluoride (PVDF) membranes (Invitrogen) and biotin detection using horseradish peroxidase (HRP)-conjugated streptavidin and the Supersignal West Pico Chemiluminescent kit (Pierce, ThermoFisher Scientific, Courtaboeuf, France). Signals were quantified by densitometry using ImageJ software. Statistical significance ($P < 0.05$) was tested using a Mann-Whitney U test.

Western Blotting

Fibroblasts and transfected COS7 cells were lysed in 50 mM Tris pH 7.4, 0.1% Triton X-100, 150 mM NaCl, 10% glycerol, 5 mM $MgCl_2$, 1% phosphatase inhibitor cocktails 1 and 2 (P2850 and P5726; Sigma-Aldrich, Saint Quentin Fallavier, France), and 1% protease inhibitor cocktail (P8340; Sigma-Aldrich). Twenty μg of protein extract in loading buffer (50 mM Tris-HCl, 2% SDS, 10% glycerol, 1% β-mercaptoethanol and bromophenol blue) were submitted to electrophoresis on a 10% SDS-PAGE and then transferred onto PVDF membranes. Nonspecific sites were blocked for 2 hr at room temperature in PBS with 5% nonfat dry milk and 0.1% Triton X-100. Incubation with primary antibody was performed overnight at 4°C with antibodies against ERK1 and ERK2 (C-16, 1:400; Santa Cruz Biotechnology), phosphorylated ERK1 and ERK2 (E-4, 1:400; Santa Cruz Biotechnology), phosphorylated MEK1 and MEK2 (Ser 218/Ser 222, 1:400; Santa Cruz Biotechnology), DNM2 (C18-goat polyclonal antibody, 1:400; Santa Cruz Biotechnology), TR (ab65831-rabbit polyclonal antibody, 1:200; Abcam) or GFP (FL, 1:200; Santa Cruz Biotechnology) and 1 hr at room temperature with an antibody against the α-tubulin (mouse monoclonal antibody, 1:1000; Sigma Aldrich). After washing, membranes were incubated 2 hr at room temperature with HRP-conjugated secondary antibodies (anti-goat-HRP from Jackson ImmunoResearch [Suffolk, UK], anti-mouse-HRP or anti-rabbit-HRP [both from Dako, Trappes, France]) diluted at 1:2000 in blocking buffer. Detection was performed using the Supersignal West Pico Chemiluminescent kit (Pierce). In ERK activation experiments, fibroblasts and transfected COS7 cells were incubated with EGF (10 ng/ml) for 5 min and rapidly washed in PBS before lysis. Signals were quantified by densitometry using the Genetools software (Syngene, Cambridge, UK). Statistical significance ($P < 0.05$) was tested using a Mann-Whitney U test.

Detection of Tyrosine-Phosphorylated Proteins With Antibody Microarrays

Protein extracts from healthy controls and CNM fibroblasts were performed as above. A PhosphoMagyArray (ProtNeteomix, Nantes, France) was prepared by immobilization of 120 monoclonal antibodies generated against target proteins onto nitrocellulose membrane FAST-slide (Whatman–GE Healthcare, Orsay, France). The microarrays contain control microspots including tyrosine-phosphorylated bovine serum albumin (BSA) used for normalization of signal intensity. The slides were incubated in TBST (50 mM Tris pH 7.2, 137 mM NaCl, 0.1% Tween-20) supplemented with 5% BSA at 4°C for 1 hr. The slides were washed with TBST three times for 5 min at room temperature. Cell extracts were added at 0.5 mg/ml total protein concentration in TBST supplemented with 1% BSA and the incubation was continued at 4°C overnight. After washing with TBST, the slides were incubated with 1.5 μg/ml biotinylated phosphotyrosine mouse monoclonal antibody (P-Tyr-100; Cell Signaling Technology, Boston, MA) at room temperature for 1 hr and then washed again and incubated with streptavidin, AlexaFluor 680 (Invitrogen) at 5 μg/ml in TBST at room temperature for 1 hr. After three washings, the slides were scanned with an Odyssey infrared imaging system (LI-COR Biosciences, Lincoln, NE) using near-infrared fluorescence excitation (700 nm) providing higher sensitivity on a nitrocellulose membrane to detect antibody–protein interactions [Snapyan et al., 2003].

Results

A Novel CNM Mutation in the GED

In a large CNM family originating from Chile, we identified the first mutation in the DNM2 GED. The mutation (c.1948G > A) induces the change of glutamate 650 to lysine (p.E560 K) (Supp. Fig. S1). The mutation was not found in the healthy members of the family nor in 100 unrelated healthy subjects, and affects a conserved residue within the human dynamin family and orthologs from different species (Supp. Fig. S1). Clinically, the five patients presented a moderate myopathy beginning during childhood with normal or delayed motor milestones (two patients walked after the age of 2 years). All the patients presented with ptosis from childhood but no oculomotor impairment. After the second decade, the myopathy showed a slowly progressive course with facial and neck muscle weakness and distal lower limb atrophy in the anterolateral compartment of the legs. Serum creatine phosphokinase (CK) levels were normal, and electrophysiological evaluation was normal or showed only unspecific myopathic changes. No cardiac or respiratory involvement was observed. Deep tendon reflexes were decreased or absent in three of the patients, and mental retardation was present in one patient.

DNM2 Isoforms in Human Tissues

Four different DNM2 isoforms are expressed from the *DNM2* gene by the combined use of two alternative splice sites (Supp. Fig. S2). Isoforms 1, 2, 3, and 4 are also known as isoforms aa, ba, ab, and bb, respectively. Exon 10 and 10bis have the same length (139 bp–identity 70%) and are alternatively spliced. Exon 13bis (12 bp) is spliced or retained, leading to the translation of proteins of 866 (isoforms 3 and 4) or 870 amino acids (isoforms 1 and 2). An RT-PCR assay was developed using a single pair of primers for the coamplification of the four isoforms and the subsequent discrimination of the isoforms by enzyme digestion and gel electrophoresis. Using this approach, we showed that the four DNM2 isoforms are expressed both in human skeletal muscle and peripheral nerve (Supp. Fig. S2).

Clathrin-Mediated Receptor Endocytosis Assay

We tested the capability of three CNM-DNM2 mutations (p.R465W, p.V625del, and p.E650 K) and of one CMT-DNM2 mutation (p.K562E) to inhibit clathrin-mediated receptor endocytosis. The point mutation, p.K44A, defective for GTPase activity, was used as a control of inhibition [Damke et al., 1994]. The GFP-DNM2-wild-type fluorescence in the transfected COS7 cells (Figs. 1 and 2) appears similar to the endogenous DNM2 immunostaining in COS7 cells illustrated in Figure 1, both showing a diffuse staining of the cytoplasm. Receptor endocytosis was first assessed by fluorescent-transferrin uptake after 5 and 15 min of incubation (Fig. 1). In COS7 cells transfected with wild-type DNM2, internalized transferrin is visible after 5 min incubation and accumulates in a juxtanuclear region after 15 min. In cells transfected with the dominant negative p.K44A mutant, transferrin uptake is strongly inhibited at 5 and 15 min. Transferrin uptake is also decreased in cells expressing the DNM2 mutants p.R465W, p.K562E, and p.E650 K at 5 and 15 min. Inhibition of the uptake appears lower in cells transfected with the p.V625del mutant after 5 min, but the juxtanuclear accumulation of transferrin still has not occurred after 15 min. At this time, quantification of the transferrin-associated signal in the transfected cells (Fig. 3A) indicates that uptake is significantly decreased in cells overexpressing the DNM2-mutants by comparison with the wild-type transfected cells. In order to confirm inhibition of clathrin-mediated endocytosis resulting from the overexpression of DNM2 mutants, we assessed the capability of the same DNM2 mutants to inhibit uptake of fluorescent LDL, another marker of clathrin-mediated receptor endocytosis. DiI-LDL uptake was assessed after 15 min of incubation (Fig. 2). A juxtanuclear accumulation of the marker was achieved in cells overexpressing the wild-type DNM2. By comparison, expression of the p.K44A mutant as well as CNM and CMT mutants diminishes the fluorescent LDL uptake except for the p.R465W, which exhibits a lower inhibition. The DiI-LDL signal in transfected cells is significantly decreased in cells expressing the p.K44A, p.K562E, p.V625del, and p.E650 K mutants when compared to cells expressing the wild-type-DNM2 (Fig. 3B). Taken together, our data show that the p.E650 K CNM and the p.K562E CMT mutants induce a marked decrease of clathrin-mediated receptor endocytosis. The p.R465W and p.V625del CNM mutants are either less efficient or may have differential inhibitor effect on transferrin or LDL receptor endocytosis.

EGF-Induced ERK1 and ERK2 Activation

We studied the capability of the same DNM2-mutants to impair EGF-induced ERK1 and ERK2 (44 kDa and 42 kDa, respectively) activation in transfected COS7 cells. EGF treatment (10 ng/ml, 5 min) induces ERK1 and ERK2 activation in COS7 cells transfected with the empty plasmid, as visualized by immunoblotting using antibody against phosphorylated ERK1 and ERK2 (Fig. 4). Transfection of wild-type DNM2 does not modify EGF-induced ERK activation whereas the activation is strongly inhibited by overexpression of the dominant negative p.K44A mutant. ERK phosphorylation is also significantly decreased after expression of the CNM-DNM2 mutants, p.R465W, p.V625del, and p.E650 K, and the CMT-DNM2 mutant, p.K562E. The transfection efficiency was verified by GFP immunoblotting, which revealed a similar expression level of GFP-DNM2 chimera in both stimulated and unstimulated conditions. The total content of ERK1 and ERK2 determined in the same protein extracts is not statistically modified after a 48-hr expression of wild-type or mutant forms of DNM2 (Supp. Fig. S3). EGF-induced activation of MAPK kinase (MEK), the kinase responsible for the activation of ERK1 and ERK2, is not changed by expression of the DNM2 mutants as compared to the activation of MEK in cells transfected with the empty plasmid or cells expressing the wild-type DNM2 (Fig. 4).

DNM2 Expression in CNM Fibroblasts

The pattern of expression of the three classical dynamins was determined by RT-PCR in healthy control and CNM fibroblast cell lines. Human fibroblasts express DNM1 and DNM2 transcripts, and only express DNM3 at a very low level. BsaMI digestion of the DNM2 amplicons shows that fibroblasts mainly express DNM2 isoforms 1 and 2 (Supp. Fig. S4). There is no difference in the transcriptional pattern of DNM1, DNM2, and DNM3, and in DNM2 isoform content in the CNM fibroblast cell line compared to healthy control fibroblasts. DNM2 immunoblot shows similar expression levels in CNM and control fibroblasts (Supp. Fig. S4). In control and CNM fibroblasts, DNM2 immunolabeling is diffuse in the cytoplasm (Supp. Fig. S4). These results indicate that in p.R465W fibroblasts, the mutated DNM2 is expressed at a normal level and its localization is not modified.

Transferrin Uptake and EGF Stimulation in CNM Fibroblasts

The uptake of biotinylated-transferrin was quantified after 5 min of incubation in one CNM fibroblast cell line expressing the p.R465W. The uptake in the CNM fibroblasts is significantly decreased when compared to the values of the two control cell lines (Fig. 5A). No difference in transferrin receptor expression or localization was observed between control and CNM fibroblasts by western blotting and immunocytochemistry (Supp. Fig. S4). Stimulation of healthy control fibroblasts by EGF induces the phosphorylation of ERK1 and ERK2 after 5 min of incubation (Fig. 5B and C). The EGF-induced ERK1 and ERK2 activation and the total ERK content in the CNM-fibroblast cell line are close to the values in the two control lines. To confirm this result and assess the impact of DNM2 mutations in fibroblasts on the phosphorylation of other proteins, we used PhosphoMagyArrays (ProtNeteomix), allowing quantification of the phosphorylation level of 120 proteins engaged in the regulation of cell cycle, cytoskeleton, and several signaling pathways. After EGF stimulation at 10 ng/ml and 150 ng/ml for 5 min, no significant change in phosphorylation levels was seen in the CNM fibroblast cell line when compared with the two healthy controls for any of the proteins analyzed, including proteins of the MAPK ERK1 and ERK2 pathway (Supp. Table S1).

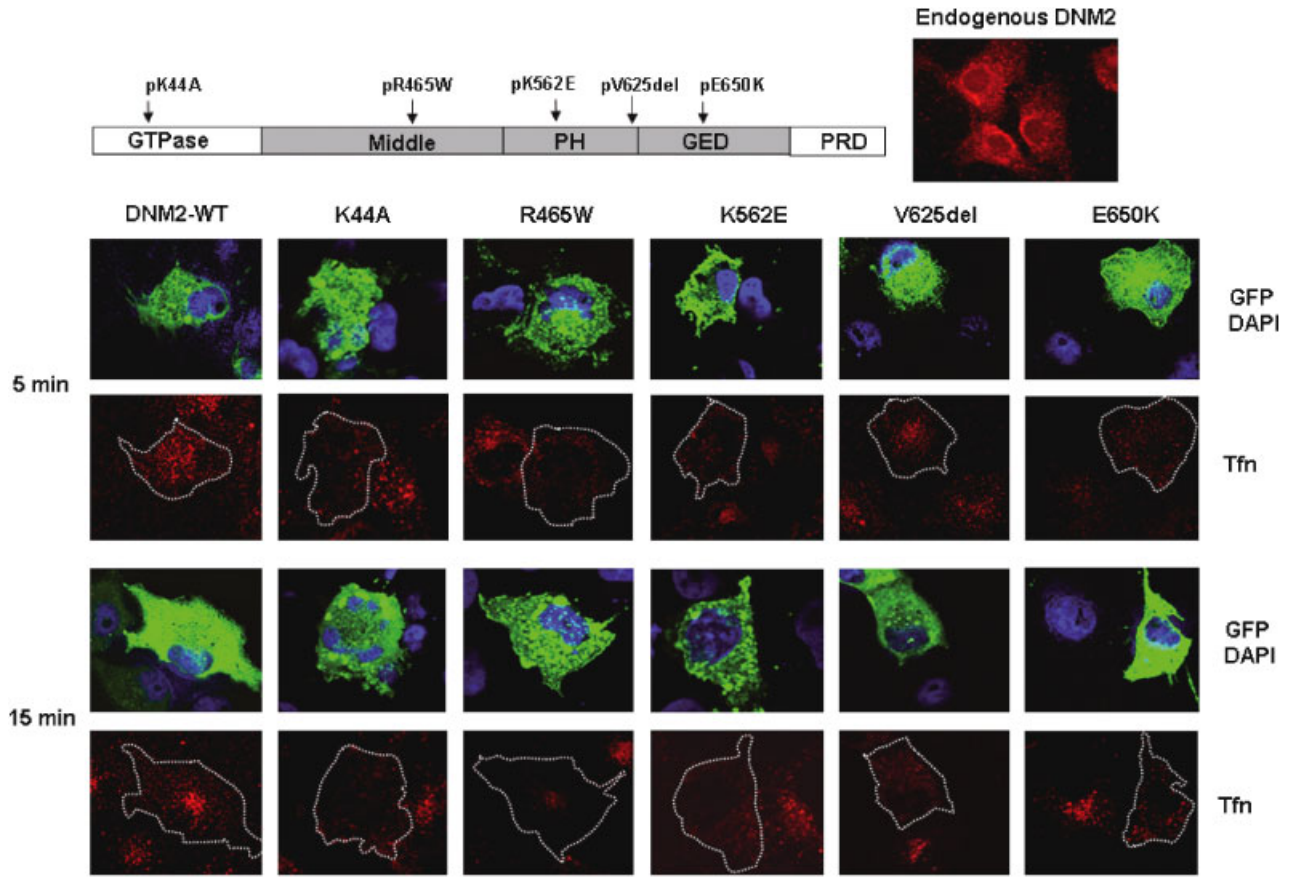

Figure 1. Transferrin uptake in COS7 cells transfected with mutant DNM2-GFP tagged constructs. The schematic representation of DNM2 shows the position of the DNM2 mutants. p.R465W, p.V625del, and p.E650 K are CNM-associated mutations and p.K562E causes CMT. p.K44A is a dominant negative mutant, defective for GTPase activity and is used as a control. The endogenous DNM2 immunostaining in COS7 cells shows diffuse staining of the cytoplasm. Representative cells are shown for fluorescent transferrin (Tfn) uptake after 5 and 15 min of incubation. Transfected cells, identified by the fluorescence of the GFP tag, are surrounded by a dotted line. 4′,6′-diamino-2-phenylindole (DAPI) was used to stain the nuclei. Transferrin was visualized by Alexa-Fluor568-fluorescence. By comparison to cells transfected with the DNM2–wild-type (WT), uptake was inhibited by p.K44A, p.R465W, p.K562E, p.E650 K after 5 and 15 min and inhibited by p.V625del after 15 min.

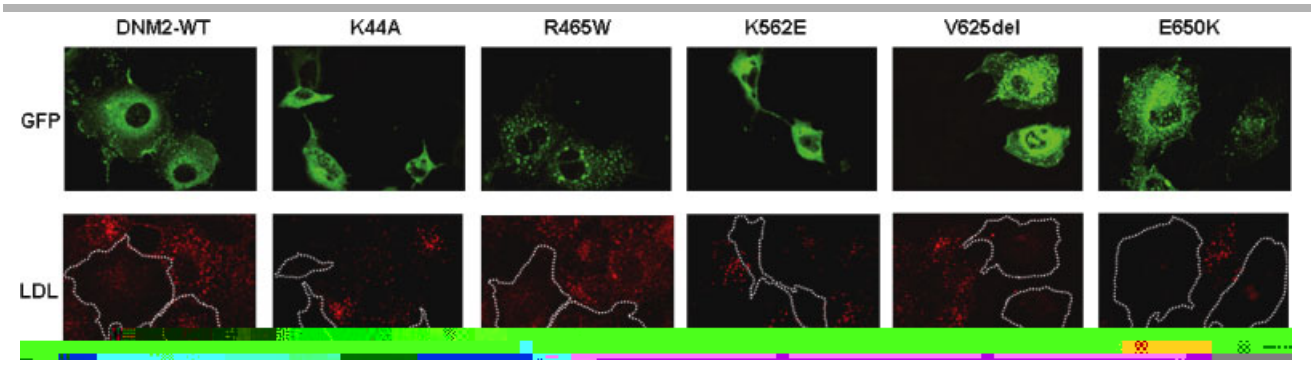

Figure 2. DiI-LDL uptake in COS7 cells transfected with mutant DNM2-GFP tagged constructs. Representative cells are shown for fluorescent LDL uptake after 15 min of incubation. Transfected cells, identified by the fluorescence of the GFP tag, are surrounded by a dotted line. By comparison to cells transfected with the DNM2—wild-type (WT), uptake was inhibited by p.K44A, p.V625del, p.K562E, and p.E650 K, and only moderately inhibited by p.R465W.

Discussion

Heterozygous *DNM2* mutations cause CNM, a rare form of congenital myopathy, and CMT, a peripheral neuropathy. In both disorders, the clinical spectrum associated with *DNM2* mutations is wide. In CNM, DNM2 mutations lead to rare severe neonatal forms and to more frequent milder forms of the disease, and in CMT, mutations are associated with both dominant intermediate and axonal forms of the disease. To date, CNM- and CMT-associated mutations have been reported in the middle and PH domains. Here, we enlarge the spectrum of CNM *DNM2* mutations by the identification of the first mutation (p.E650 K) in the GED. By comparison with the phenotypes previously described, the GED

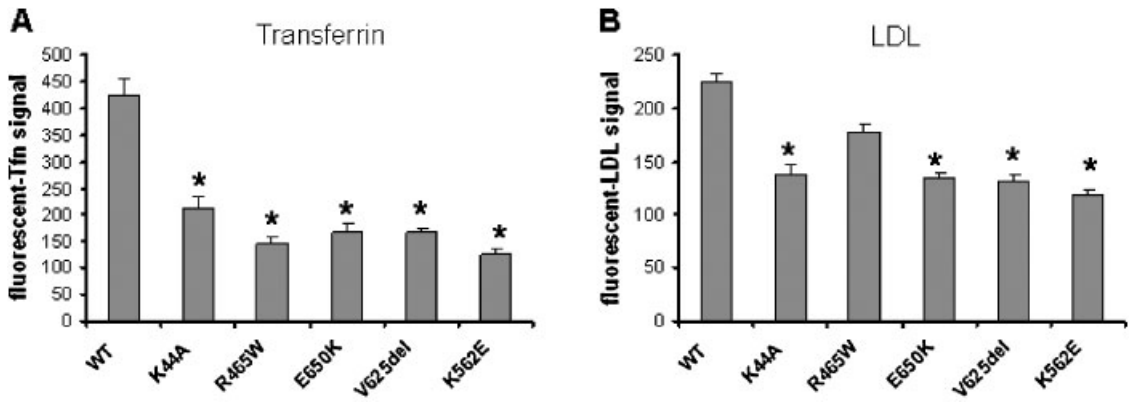

Figure 3. Quantification of the uptake of transferrin and LDL after 15 min of incubation. Confocal images were used to quantify the signal associated with the fluorescent transferrin (**A**) or fluorescent DiI-LDL (**B**) in the transfected cells identified by the GFP-associated fluorescence due to the expression of the DNM2 constructs. The histograms represent the means ± standard error of the mean (SEM) ($n = 30$ cells), $^{*}P < 0.001$ compared to the wild-type (WT) construct using a Student's *t*-test.

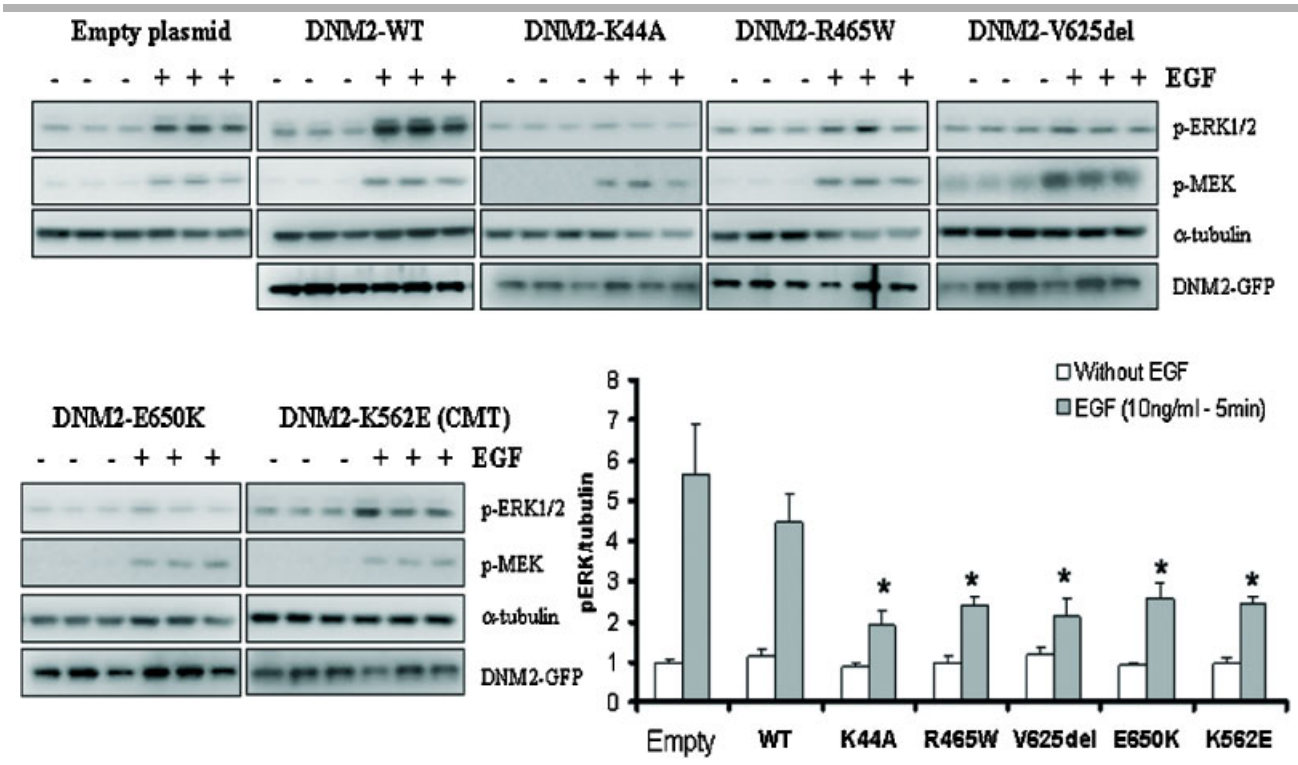

Figure 4. MAPK ERK1 and ERK2 activation in COS7 expressing DNM2 mutants. Representative western blots of transfected COS7 cells after treatment by EGF (10 ng/ml for 5 min). Phosphorylation of ERK and MEK increases in cells transfected with the empty plasmid or expressing the wild-type DNM2. In contrast, overexpression of the DNM2-mutants inhibits ERK phosphorylation, whereas activation of MEK is preserved. α-Tubulin was used as a loading control and transfection efficiency was checked by western blotting of GFP-DNM2. The pERK signal was quantified by densitometry and normalized to α-tubulin signal intensity. The histogram represents the mean ± standard error of the mean (SEM) ($n = 6$). Statistical analysis was performed using Mann-Whitney test; $^{*}P < 0.05$ vs. EGF-treated wild-type (WT) values.

mutation leads to a relatively mild phenotype comparable to those of the CNM patients harboring the two most frequent mutations in the middle domains; i.e., p.R465W and p.R369Q.

The 100-kD GTPase DNM2 is involved in clathrin-mediated and clathrin-independent endocytosis [Warnock et al., 1997; Henley et al., 1998]. DNM2 is recruited at the plasma membrane as an helical oligomer around the neck of the nascent vesicles. GTP hydrolysis induces a conformational modification of the helix leading to the fission of the neck of the vesicles. Each domain of the protein in which human mutations have been identified contributes to this process. The middle domain is involved in the self-assembly of the molecule in the helical structure [Okamoto et al., 1999; Smirnova et al., 1999]. GTPase hydrolysis, highly stimulated by self-assembly, induces a conformational change of the middle domain associated with a constriction of lipid structures [Chen et al., 2004]. The PH domain is involved in the interaction with membrane phosphoinositides, especially phosphatidylinositol 4-5 bisphosphate, and is thus involved in the targeting of dynamin to plasma membranes [Dong et al., 2000]. The GED domain both participates in the self-assembly of

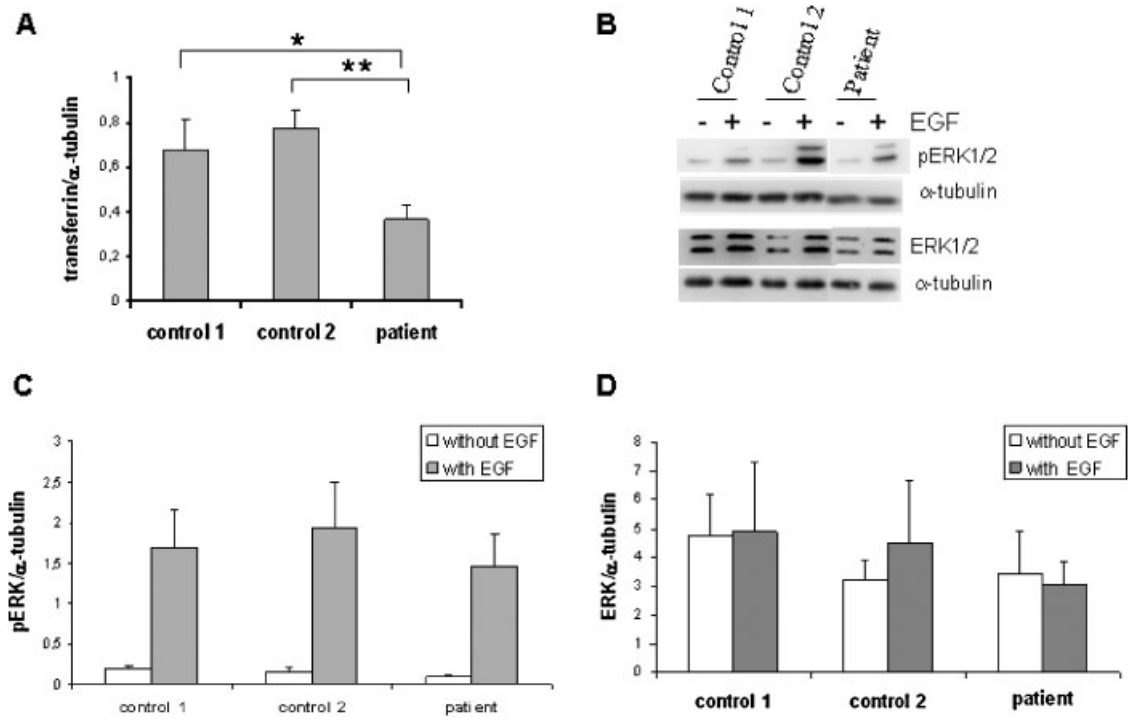

Figure 5. Transferrin uptake and EGF-induced activation of ERK1 and ERK2 in CNM patient fibroblasts. **A:** Quantification of the uptake of biotinylated-transferrin in CNM fibroblasts. Cells were incubated for 5 min with transferrin before lysis, SDS-PAGE, transfer onto PVDF membrane, and hybridization with HRP-conjugated streptavidin. Signals were quantified by densitometry. $^{*}P<0.05$ and $^{**}P<0.001$ using a Mann-Whitney U-test for CNM patient ($n=21$) vs. control 1 ($n=12$) and control 2 ($n=12$). **B:** Western blot of phosphorylated ERK1 and ERK2 and total ERK content in one CNM fibroblast cell line and two healthy control subjects after EGF treatment (10 ng/ml for 5 min). The patient harbors the p.R465W mutation. α-Tubulin was used as loading control. **C,D:** Quantification by densitometry of the signal of pERK and total ERK from two independent experiments. ERK and pERK signals were normalized using α-tubulin signal ($n=4$).

dynamins [Sever et al., 1999; Muhlberg and Schmid, 2000] and acts as a GTPase-activating protein (GAP) [Sever et al., 1999]. Among the 12 *DNM2* mutations identified in CNM, no genotype–phenotype relationship can be clearly ascertained, except that mutations in the C-terminal part of the PH domain are all associated with a severe neonatal CNM phenotype [Bitoun et al., 2007] by mechanisms which remain to be determined.

In vitro transfection of plasmids carrying DNM1 and DNM2 point mutations has largely been used to study the role of dynamins in endocytosis. In general, overexpression of DNM mutants in cell lines leads to a decrease of clathrin-mediated receptor endocytosis when visualized by fluorescent transferrin uptake. However, some exceptions exist in which a point mutation in the PH or GED domains results in no change or even an increase in transferrin uptake [Sever et al., 1999; Vallis et al., 1999]. In order to determine the effect of the DNM2 mutations associated with human diseases on clathrin-mediated endocytosis, we studied transferrin and LDL uptake in COS7 cells over-expressing three CNM-DNM2 mutations located in the MD, PH, and GED, and one CMT-DNM2 mutation in the PH domain. The tested mutants led to a similar inhibition of receptor-mediated endocytosis except for the p.R465W on the LDL uptake. In this case, the uptake of the fluorescent marker is only slightly inhibited. We have no explanation for this particular result given that the two markers enter in the cell probably use the same protein machinery. We can speculate that some differences exist in the clathrin-mediated endocytosis involved in the uptake of the two receptors and that these differences can explain the specific effect of this mutant. Nevertheless, our results show that all of the disease-associated mutants are able to inhibit one clathrin-mediated endocytosis process. Impairment of transferrin uptake was also found in CNM fibroblasts expressing the p.R465W mutation. Interestingly, homozygous mutations in the *BIN1* gene (NC_000002.10) encoding amphiphysin 2 (MIM♯ 601248) cause the autosomal recessive form of CNM [Nicot et al., 2007]. Amphiphysin 2 is a partner of DNM2 involved in the endocytosis process [Wigge and McMahon, 1998; Kojima et al., 2004], and disease-associated mutations have been shown to disrupt interaction with DNM2 [Nicot et al., 2007]. Taken together, these results suggest that alteration of clathrin-mediated endocytosis may contribute to the pathophysiological mechanisms of autosomal CNM.

Several human diseases, including leukemia and neurological disorders, have been previously associated with a defect of clathrin-coated vesicles [Floyd and De Camilli, 1998; Yao et al., 1999; Pucharcos et al., 1999]. In skeletal muscle, defects in endocytosis at the plasma membrane and in secretion from the trans-Golgi network have been implicated in the pathogenesis of distal myopathy with rimmed vacuoles [Kumamoto et al., 2000]. Clathrin-mediated endocytosis mediates sorting and selective transport of proteins involved in intracellular pathways and tightly controls the activity of G protein–coupled receptors and tyrosine kinase receptors. In particular, activation of the MAPK ERK1 and ERK2 pathway has been shown to be both endocytosis- and DNM2-dependent [Andresen et al., 2002; Kranenburg et al., 1999] probably through a membrane-associated trafficking from the plasma membrane responsible for the transport of activated MEK toward its targets; i.e., ERK1 and ERK2. Here, we report that all of the DNM2 mutants tested were able to decrease the EGF-induced activation of the ERK1 and ERK2 in transfected COS7 cells. Our

results suggest that inhibition occurs at the level of activation of ERK by MEK, as previously reported [Kranenburg et al., 1999]. In contrast, the reduced EFG-induced activation of ERKs was not observed in CNM skin fibroblasts. This result was confirmed by a protein array approach. This may indicate that the ERK pathway does not contribute to the pathomechanisms in vivo. Alternatively, DNM1 expression in human skin fibroblasts could partially compensate for DNM2 defects and allow normal ERK activation. Further studies will be necessary in human muscle cells to evaluate the possible contribution of the ERK pathway in CNM pathomechanisms.

Our results indicate that CNM-related and CMT-related DNM2 mutants, when expressed in vitro, have the same impact on clathrin-mediated endocytosis and EGF-induced ERK1 and ERK2 activation, while they induce different tissue-specific phenotypes in patients. We transfected the DNM2 isoform 1, which is expressed in human skeletal muscle and peripheral nerve. Nevertheless, as we showed in this study, the three other isoforms are also expressed in these tissues but their regulation and specific functions are not known. Investigations on these isoforms and their partners may help in the future to understand the tissue-specific phenotype of DNM2 mutations.

In conclusion, we showed that overexpression of CNM- and CMT-related DNM2 mutants in COS7 cells, whatever the mutated domain, led to a reduction in clathrin-mediated receptor endocytosis associated with MAPK ERK1 and ERK2 impairment. Our results suggest that impairment of the membrane trafficking process may represent a common pathophysiological pathway in the autosomal forms of CNM and DNM2-CMT neuropathy.

Acknowledgments

We thank the Institut National de la Santé et de la Recherche Médicale (INSERM), the Association Française contre les Myopathies (AFM) for financial support, the Laboratoire de Neuropathologie de l'Hôpital Pitié-Salpêtrière for providing the peripheral nerve sample, and M. Bromberg for performing the muscle and skin biopsy on one of the families. J.A.B. was supported by the Programme Alban, the European Union Programme of High Level Scholarships for Latin America, scholarship No. E04E028343CL. A.-C.D. was a recipient of Région Ile-de-France and AFM fellowships.

References

Andresen BT, Rizzo MA, Shome K, Romero G. 2002. The role of phosphatidic acid in the regulation of the Ras/MEK/Erk signaling cascade. FEBS Lett 531:65–68.

Bitoun M, Maugenre S, Jeannet PY, Lacène E, Ferrer X, Laforêt P, Martin JJ, Laporte J, Lochmüller H, Beggs AH, Fardeau M, Eymard B, Romero NB, Guicheney P. 2005. Mutations in dynamin 2 cause dominant centronuclear myopathy. Nat Genet 37:1207–1209.

Bitoun M, Bevilacqua JA, Prudhon B, Maugenre S, Taratuto AL, Monges S, Lubieniecki F, Cances C, Uro-Coste E, Mayer M, Fardeau M, Romero NB, Guicheney P. 2007. Dynamin 2 mutations cause sporadic centronuclear myopathy with neonatal onset. Ann Neurol 62:666–670.

Bitoun M, Stojkovic T, Prudhon B, Maurage CA, Latour P, Vermersch P, Guicheney P. 2008. A novel mutation in the dynamin 2 gene in a Charcot-Marie-Tooth type 2 patient: clinical and pathological findings. Neuromuscul Disord 18:334–338.

Bitoun M, Bevilacqua JA, Eymard B, Prudhon B, Fardeau M, Guicheney P, Romero NB. 2009. A new centronuclear myopathy phenotype due to a novel Dynamin 2 mutation. Neurology 72:93–95.

Cartier L, Hernandez JE. 1996. [Late centronuclear myopathy: autosomal dominant form]. Rev Med Chil 124:209–216.

Chen YJ, Zhang P, Egelman EH, Hinshaw JE. 2004. The stalk region of dynamin drives the constriction of dynamin tubes. Nat Struct Mol Biol 11:574–575.

Cook TA, Urrutia R, McNiven MA. 1994. Identification of dynamin 2, an isoform ubiquitously expressed in rat tissues. Proc Natl Acad Sci USA 91:644–648.

Damke H, Baba T, Warnock DE, Schmid SL. 1994. Induction of mutant dynamin specifically blocks endocytic coated vesicle formation. J Cell Biol 127:915–934.

Diatloff-Zito C, Gordon AJ, Duchaud E, Merlin G. 1995. Isolation of an ubiquitously expressed cDNA encoding human dynamin II, a member of the large GTP-binding protein family. Gene 163:301–306.

Dong J, Misselwitz R, Welfle H, Westermann P. 2000. Expression and purification of dynamin II domains and initial studies on structure and function. Protein Expr Purif 20:314–323.

Echaniz-Laguna A, Nicot AS, Carre S, Franques J, Tranchant C, Dondaine N, Biancalana V, Mandel JL, Laporte J. 2007. Subtle central and peripheral nervous system abnormalities in a family with centronuclear myopathy and a novel dynamin 2 gene mutation. Neuromuscul Disord 17:955–959.

Fabrizi GM, Ferrarini M, Cavallaro T, Cabrini I, Cerini R, Bertolasi L, Rizzuto N. 2007. Two novel mutations in dynamin-2 cause axonal Charcot-Marie-Tooth disease. Neurology 69:291–295.

Fischer D, Herasse M, Bitoun M, Barragán-Campos HM, Chiras J, Laforêt P, Fardeau M, Eymard B, Guicheney P, Romero NB. 2006. Characterization of the muscle involvement in dynamin 2- related centronuclear myopathy. Brain 129:1463–1469.

Floyd S, De Camilli P. 1998. Endocytosis proteins and cancer: a potential link? Trends Cell Biol 8:299–301.

Gallardo E, Claeys KG, Nelis E, García A, Canga A, Combarros O, Timmerman V, De Jonghe P, Berciano J. 2008. Magnetic resonance imaging findings of leg musculature in Charcot-Marie-Tooth disease type 2 due to dynamin 2 mutation. J Neurol 255:986–992.

Henley JR, Krueger EW, Oswald BJ, McNiven MA. 1998. Dynamin-mediated internalization of caveolae. J Cell Biol 141:85–99.

Jeannet PY, Bassez G, Eymard B, Laforet P, Urtizberea JA, Rouche A, Guicheney P, Fardeau M, Romero NB. 2004. Clinical and histologic findings in autosomal centronuclear myopathy. Neurology 62:1484–1490.

Jones SM, Howell KE, Henley JR, Cao H, McNiven MA. 1998. Role of dynamin in the formation of transport vesicles from the trans-Golgi network. Science 279:573–577.

Kojima C, Hashimoto A, Yabuta I, Hirose M, Hashimoto S, Kanaho Y, Sumimoto H, Ikegami T, Sabe H. 2004. Regulation of Bin1 SH3 domain binding by phosphoinositides. EMBO J 23:4413–4422.

Kranenburg O, Verlaan I, Moolenaar WH. 1999. Dynamin is required for the activation of mitogen-activated protein (MAP) kinase by MAP kinase kinase. J Biol Chem 274:35301–35304.

Kumamoto T, Ito T, Horinouchi H, Ueyama H, Toyoshima I, Tsuda T. 2000. Increased lysosome-related proteins in the skeletal muscles of distal myopathy with rimmed vacuoles. Muscle Nerve 23:1686–1693.

Muhlberg AB, Schmid SL. 2000. Domain structure and function of dynamin probed by limited proteolysis. Methods 20:475–483.

Nakata T, Takemura R, Hirokawa N. 1993. A novel member of the dynamin family of GTP-binding proteins is expressed specifically in the testis. J Cell Science 105:1–5.

Nicot AS, Toussaint A, Tosch V, Kretz C, Wallgren-Pettersson C, Iwarsson E, Kingston H, Garnier JM, Biancalana V, Oldfors A, Mandel JL, Laporte J. 2007. Mutations in amphiphysin 2 (BIN1) disrupt interaction with dynamin 2 and cause autosomal recessive centronuclear myopathy. Nat Genet 39:1134–1139.

Okamoto PM, Tripet B, Litowski J, Hodges RS, Vallee RB. 1999. Multiple distinct coiled-coils are involved in dynamin self-assembly. J Biol Chem 274:10277–10286.

Orth JD, McNiven MA. 2003. Dynamin at the actin-membrane interface. Curr Opin Cell Biol 15:31–39.

Praefcke GJ, McMahon HT. 2004. The dynamin superfamily: universal membrane tubulation and fission molecules? Nat Rev Mol Cell Biol 5:133–147.

Pucharcos C, Fuentes JJ, Casas C, de la Luna S, Alcantara S, Arbones ML, Soriano E, Estivill X, Pritchard M. 1999. Alu-splice cloning of human Intersectin (ITSN), a putative multivalent binding protein expressed in proliferating and differentiating neurons and overexpressed in Down syndrome. Eur J Hum Genet 7:704–712.

Schessl J, Medne L, Hu Y, Zou Y, Brown MJ, Huse JT, Torigian DA, Jungbluth H, Goebel HH, Bonnemann CG. 2007. MRI in DNM2-related centronuclear myopathy: evidence for highly selective muscle involvement. Neuromuscul Disord 17:28–32.

Sever S, Muhlberg AB, Schmid SL. 1999. Impairment of dynamin's GAP domain stimulates receptor-mediated endocytosis. Nature 398:481–486.

Shpetner HS, Vallee RB. 1989. Identification of dynamin, a novel mechanochemical enzyme that mediates interactions between microtubules. Cell 59:421–432.

Smirnova E, Shurland DL, Newman-Smith ED, Pishvaee B, van der Bliek AM. 1999. A model for dynamin self-assembly based on binding between three different protein domains. J Biol Chem 274:14942–14947.

Snapyan M, Lecocq M, Guevel L, Arnaud MC, Ghochikyan A, Sakanyan V. 2003. Dissecting DNA-protein and protein-protein interactions involved in bacterial transcriptional regulation by a sensitive protein array method combining a near-infrared fluorescence detection. Proteomics 3:647–657.

Thompson HM, Cao H, Chen J, Euteneuer U, McNiven MA. 2004. Dynamin 2 binds gamma-tubulin and participates in centrosome cohesion. Nat Cell Biol 6:335–342.

Vallis Y, Wigge P, Marks B, Evans PR, McMahon HT. 1999. Importance of the pleckstrin homology domain of dynamin in clathrin-mediated endocytosis. Curr Biol 9:257–260.

Warnock DE, Baba T, Schmid SL. 1997. Ubiquitously expressed dynamin-II has a higher intrinsic GTPase activity and a greater propensity for self-assembly than neuronal dynamin-I. Mol Biol Cell 8:2553–2562.

Wigge P, McMahon HT. 1998. The amphiphysin family of proteins and their role in endocytosis at the synapse. Trends Neurosci 21:339–344.

Yao PJ, Morsch R, Callahan LM, Coleman PD. 1999. Changes in synaptic expression of clathrin assembly protein AP180 in Alzheimer's disease analysed by immunohistochemistry. Neuroscience 94:389–394.

Yoo J, Jeong MJ, Cho HJ, Oh ES, Han MY. 2005. Dynamin II interacts with syndecan-4, a regulator of focal adhesion and stress-fiber formation. Biochem Biophys Res Commun 328:424–431.

Züchner S, Noureddine M, Kennerson M, Verhoeven K, Claeys K, De Jonghe P, Merory J, Oliveira SA, Speer MC, Stenger JE, Walizada G, Zhu D, Pericak-Vance MA, Nicholson G, Timmerman V, Vance JM. 2005. Mutations in the pleckstrin homology domain of dynamin 2 cause dominant intermediate Charcot-Marie-Tooth disease. Nat Genet 37:289–294.